Nature Journal of Emerging Sciences, Technologies, & Innovations
https://naturerust.com/index.php/njesti
Vol. 6, No. 3, March 2026, pp. 315 - 336
ISSN (Print): 3115-4611, ISSN (Online): 3122-1017
DOI: https://doi.org/10.65752/eq1tse55

RESEARCH

OPEN ACCESS

An optimized deep neural network and transfer learning approaches for endometriosis classification

Opeyemi Aderiike Abisoye[1,3]*, Ruth Ailoyafen[1], Solomon Adelowo Adepoju[1], Blessing Olatunde Abisoye[2], Oladayo Tosin Akinwande[3], Ikouwen Ufort Usoh[3]

[1]Department of Computer Science, Federal University of Technology, Minna, Nigeria.
[2]Department of Computer Engineering, Federal University of Technology, Minna, Nigeria.
[3]Department of Software Engineering, Veritas University, Abuja, Nigeria.

Article Info

Article history:

Received: February 10th 2026
Revised: March 3rd 2026
Accepted: March 13th 2026

ailoyafenruth@gmail.com
https://orcid.org/0009-0000-8471-3593
(Ailoyafen R.)
solo.adepoju@futminna.edu.ng
https://orcid.org/(0000-0002-1128-4753
(Adepoju S.A.)
b.abisoye@futminna.edu.ng
https://orcid.org/0000-0003-2750-7883
(Abisoye B.O.)
akinwandeo@veritas.edu.ng
https://orcid.org/0000-0003-4496-1885
(Akinwande O.T.)
usohi@veritas.edu.ng
https://orcid.org/0009-0005-6361-7205
(Usoh I.U.)

Keywords:

Endometriosis
Laracsopy
Transfer Learning
ResNet101V2
MobileNet
VGG16
Classification

ABSTRACT

The prevalence of endometriosis is underestimated because of the need for laparoscopy an invasive diagnostic method, which is considered the gold standard. Advanced stages of endometriosis may lead to endometrial cancer, infertility, psychological depression, leading to further complications. Endometriosis has multiple appearances; the lesions may be confused with other non-endometriotic lesions or endometriotic lesions that are non-endometriotic by appearance, or deep infiltrating ones may be missed on visual diagnosis. Therefore, this research aims to develop an endometriosis prediction by utilizing four different deep and transfer learning architecture including CNN, RestNet101V2, MobileNet, and VGG16 The proposed model employs Pelican Optimization Algorithm (POA) to extract predominant features for CNN, ResNet101V2, MobileNet, and VGG16 endometriosis classification. Image Dataset was obtained from Gynecologic Laparoscopy Endometriosis (GLENDA) repository containing 25,683 sample laparoscopic images of both pathological and non-pathological identified endometriosis regions. The experimental analysis revealed that POA_ResNet101V2, POA_MobileNet, and POA_VGG16 perform significantly better than CNN during the classification of endometriosis (pathology and non-pathology). Betterstill, MobileNet achieved a general accuracy of 100%, precision 99.5%, Recall 99.5%, and F1-score of 100%. The model demonstrates the effectiveness of transfer learning, MobileNet better than other transfer Learning in the existing studies. To address the diagnostic challenges of endometriosis, this study developed an optimized endometriosis prediction model with deep and transfer learning techniques, perform comparative analysis on the developed model and benchmark the results with existing ones. This model will assist health practitioners to early detect endometriosis and proffer appropriate solutions for patients.

*Corresponding Author

Abisoye O.A., Email: o.abisoye@futminna.edu.ng, ORCID: https://orcid.org/0000-0002-7324-2479

1. INTRODUCTION

Endometriosis is a common gynecological problem that occurs in women of aged 18 to 50 years. The lesion-like structure that underlines the uterus and other surrounding regions is referred to as endometriosis. The affected tissue is usually found on the ovaries, fallopian tubes, outer surface of the uterus and on organs within the pelvis region. It can cause pain, heavy bleeding during periods, discomfort and fertility problems. [1] stated that endometriosis is more common and more severe than it was 30 years ago. Patients with endometriosis frequently experience infertility and chronic pelvic pain [9],[34],[35]. Infertility can affect up to 30% to 50% of endometriosis-affected women. Endometriosis can affect fertility in a number of ways, including by distorting the pelvic anatomy, adhesions, scarring the fallopian tubes, inflaming the pelvic structures, altering immune system function, changing the hormonal environment of the eggs, impairing pregnancy implantation, and altering egg quality [11]. This infertility frequently goes undiagnosed because of a delay in treatment, which adds a lot of stress to the situation. Chronic pelvic pain is also reported by more than 60% of endometriosis-diagnosed women; endometriosis patients are 13 times more likely to feel abdominal pain than healthy people [2],[3],[10].

Endometriosis is a major issue, not just from a medical and social perspective but also from an economic one. Endometriosis treatment expenses in Europe range from €0.8 billion to €12.5 billion annually, depending on the nation, and are equivalent to those of other chronic diseases like diabetes. Endometriosis is also a serious social and financial burden in the US that directly and indirectly costs the country's economy $22 billion a year in lost productivity [4]. Endometriosis symptoms include the following: gradual aggravating acute premenstrual pain; abdominal pain; pain in the sacrum region of the spine; dysmenorrhea; painful ovulation; pain during sexual activity; pain when defecating and urinating; pain radiating to the back; excessive irregular menstruation; blood in the stool; gastrointestinal issues such as diarrhea or constipation; infertility; and persistent fatigue. Additionally, patients could experience unusual accompanying symptoms such as sub-febrile conditions, emotional effects, vomiting, headaches, and dizziness as well as signs of anxiety and depression, low blood sugar, bleeding from the rectal area, hematuria (Blood in urine) during periods, and allergy and infection sensitivity [3],[5].

The average time of diagnosis for women with endometriosis was estimated to be five (5) years from the symptoms onset. This delay in diagnosis can lead to a delay in treatment and can have a negative impact on the Quality of Life (QoL) of women with this condition [12][38]. Laparoscopy remains the widely used method to visualize suspicious lesions and confirm the diagnosis of endometriosis in patients [13]. Video-assisted laparoscopy (VALS) has been used for the detection and diagnosis of endometriosis [14]. It involves the insertion of a laparoscope, a thin tube with a camera and light, through a small incision in the abdomen. The camera provides a three-dimensional view of the pelvic organs, allowing the surgeon to identify and remove endometrial implants [15]. Through laparoscopic procedure, images can be viewed with more visual clarity i.e. both posterior and anterior position images can be viewed for locating the exact position of endometriosis [16][36]. But Interpretation of medical images such as CT and MRI requires extensive training and skills because the segmentation of organs and lesions needs to be performed layer by layer [17],[39],[40].

Artificial intelligence (AI) has been applied in medicine through risk assessment models, improving diagnostic accuracy, and workflow efficiency. AI systems are now capable of analyzing complex algorithms and self-learning, which has led to a new age in medicine where AI can be applied to clinical practice [6]. Machine learning technology provides a strong foundation in the medical industry, allowing for the effective diagnosis of healthcare concerns [7]. Machine learning techniques come in a variety of forms, including unsupervised, semi-supervised, supervised, reinforcement learning, evolutionary learning, and deep learning [8],[33].

Deep Learning has made significant advancements and tremendous performance in biological image classification, computer vision and cancer detection [18]. A key area of Machine Learning (ML) is Deep Learning (DL). DL models do have several benefits compared to conventional ML techniques for the classification of imagery, object identification and recognition [19],[37]. Convolutional Neural Networks (CNNs) are a type of deep learning neural network that is effective for image classification and recognition tasks [16].

`

1.1 Contribution to Knowledge

This study developed an optimized endometriosis prediction model for predicting if a patient is pathological and not pathological by utilizing four different deep and transfer learning architecture including CNN, RestNet101V2, MobileNet, and VGG16. After development an extensive comparative analysis is conducted to properly evaluate the performance of the developed prediction model. A comprehensive study is conducted to benchmark the developed model with existing baseline literatures to ascertain the research gaps and efficiency of the developed model.

Section 1 gives the introduction of the study. Section 2 reviewed several baseline Literatures. Section 3 explores the methodology of the study. Section 4 gives details of the Results and Discussions, Comparative Analysis while the Conclusion and further recommendations are provided in Section 5.

2. LITERATURE REVIEW

Sankaravadivel and Thalavipillai in 2021 [20] employed chi-square and correlation coefficients statistical methods to identify symptoms correlated with various endometriosis if the derived value is greater than 1. The algorithm had an accuracy of 90%, sensitivity 95%, specificity 78.12% and precision 90%. A self-diagnostic tool that predicts the likelihood of endometriosis based on experienced symptoms was developed by Goldstein and Cohen in 2023 [21]. Goldstein and Cohen [21] applied Decision Trees algorithm, Random Forest algorithm, Gradient Boosting Classifier (GBC) and Adaptive Boosting (AdaBoost) algorithm to train multiple endometriosis prediction models. the results showed that AdaBoost model obtained the best results with a sensitivity value of 0.939, specificity value of 0.934, precision value of 0.944 and F1-score of 0.941.

Visalaxi and Sudalai in 2021 [16] proposed a method for automated prediction of endometriosis using deep learning methods. An overall of 6000 laparoscopic data comprising of pathological and non-pathological images were taken as input. The study used Convolutional Neural Networks (CNNs) for image classification and ResNet50 architecture for transfer learning. The model achieved a training accuracy of 91%, validation accuracy of 90%, precision of 83%, specificity(recall) of 82% and Area Under Curve (AUC) of about 0.78 [16]. Balica in 2023 [22] used deep learning method to classify endometriosis from ultrasound data. The authors designed and trained five different convolutional neural network (CNN) architectures: Xception, Inception-V4, ResNet50, DenseNet and EfficientNetB2. The Densenet CNN algorithm successfully detected the presence of endometriosis on ultrasound with an AUC of 90% and an accuracy of 80% using heterogeneous patterns of endometriosis

Zhang in 2021 [22] study developed the first CNN-based Computer-Aided Diagnosis (CAD) System for classifying endometrial lesions using hysteroscopic images as input. The CNN model VGGNet-16 achieved an accuracy of 80.8% in classifying endometrial lesions, which the authors reported was slightly better than the diagnostic performance of the three gynecologists who participated in study. Hu in 2023[25], developed a deep learning model based on ultrasound (US) images to distinguish between tubal-ovarian abscess (TOA) and ovarian endometriosis cyst (OEC). Three CNN models, ResNet-152, DenseNet-161, and EfficientNet-B7, were used to differentiate TOA from OEC, and their performance was compared with three Ultra-sound physicians and a clinical indicator of carbohydrate antigen 125 (CA125). The models were trained on a dataset of 202 patients who underwent US scanning and confirmed TOA or OEC by pathology. Among the three CNN models, the performance of ResNet-152 was the highest, with Area Under the ROC Curve (AUROC) of 0.986. The AUROCs of the three physicians were 0.781, 0.738, and 0.683, respectively. The clinical indicator CA125 achieved only 0.564.

A method for automatic segmentation of the exact location of endometriosis using deep learning technique was proposed by Visalaxi in 2022 [23]. The proposed method known as Structural Similarity Analysis of Endometriosis (SSAE), identifies affected regions using U-Net architecture and a systematic sampling procedure. The SSAE implements the U-Net architecture for segmenting endometriosis based on the region of occurrence. The performance of semantic segmentation was

validated using Intersection Over Union (IOU) and F1 score. The IOU value obtained was 0.72 and the F1 score was 0.74 for the trained datasets.

The remarkable versatility of machine vision manifests across industries fueling an array of applications that elevate various domains. The healthcare realm has witnessed a transformation where machine vision evolved from a mere tool to an indispensable cornerstone in medical image analysis [27]. Deep Convolutional Networks have been very useful in machine vision tasks. These network are superior as a result of their ability to generate robust and valuable semantic features from their input data [28]. In this paper the main focus of the deep network is to classify the GLENDA datasets into pathology and nonpathology categories.

ResNet50v2 [28], VGG [32], Xception [30], Inception [30] and DenseNet [31] are the widely used deep convolutional networks. ResNet50v2 is a modified version of ResNet50 and out performs ResNet50 and ResNet 101 on the imageNet dataset [28]. ResNet50v2s madeup of 50 layers. Its architecture is b uilt upon the concept of residual learning.Resnet50v2 introduces pre-activaton residual units. Batch normalzaton and ReLU activation are applied before each convolutional layer and this helps reduce the problem of degradation often encountered n very deep networks there by improving training convergence. Resnet50v2 employs bottlenec blocs consisting of a 1x1 convolutional layer, 3x3 convolutional layer and another 1x1 convolutional layer. The shortcut connections n Resnet50v2 allows gradient problem to directly flow through the network hence, reducing the vanishing gradient problem which allows for very deep networks to be trained.

3. METHODOLOGY

This section introduces the conceptual framework and various deep learning model algorithm considered for building the endometriosis classification model.

3.1 System Design

The proposed system begins with the image loading to prediction output. Firstly, endometriosis image samples are loaded along with the trained prediction model. The image is then analyzed by the prediction model. The outcome of the analysis is a probability distribution of positive or negative outcomes.

3.1.1 System Architecture

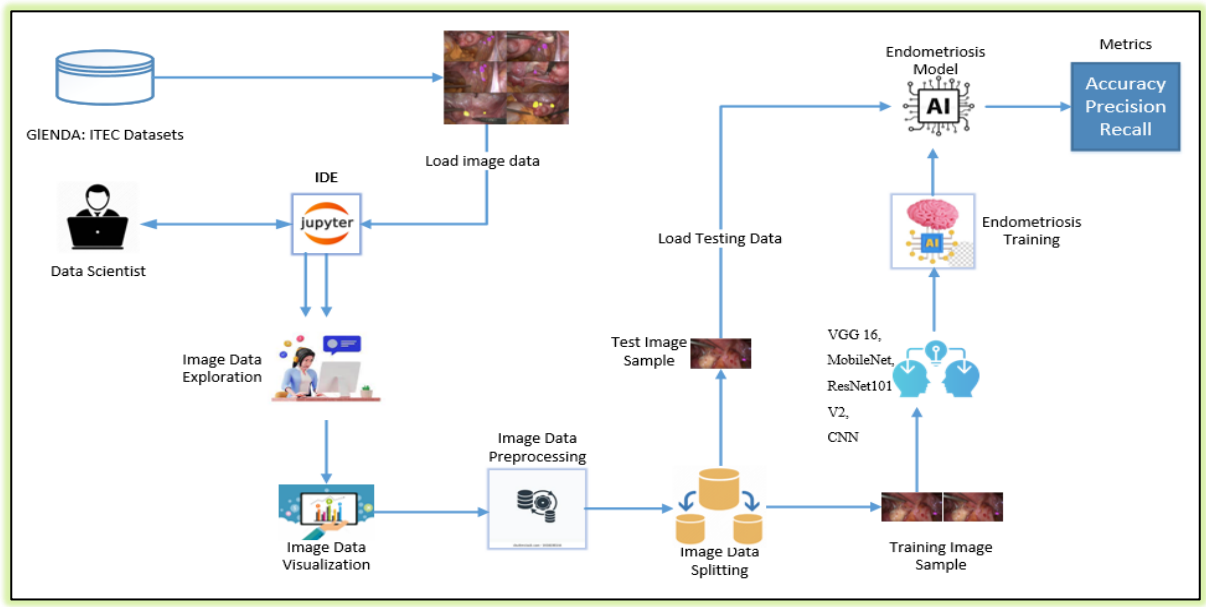

Fig.1: Conceptual design of the proposed endometriosis prediction model

Fig.1 depicts the conceptual design of the proposed endometriosis prediction model. Endometriosis dataset is downloaded from GLENDA ITEC repository and the image samples are loaded to the development kits. Data Analysis was conducted to process and vizualize the image samples by synchronizing all the image size, executing scaling operation to reduce the computation cost and improve model training performance. Hold Out

Cross validation of image data splitting into training sample (80%) and testing samples (20%) was employed to train these deep learning architecture: ResNet101V2, VGG16, MobileNet and CNN.

3.1.2. *Dataset*

The data used in this study was Laparoscopic images and annotated images of endometriosis obtained from the standardized Gynecologic Laparoscopy Endometriosis Dataset (GLENDA) v1.5 datasets [24]. The images were obtained from a video stream of Laparoscopic surgery procedure. The downloaded dataset contains 25,683 sample laparoscopic images of both pathological and non-pathological identified endometriosis regions. The data size of the endometriosis dataset is distributed as patient with pathology are of 12,244 sample images and 13,438 samples. Fig.2(a) and Fig.2(b) shows one of the images from the endometriosis Pathology class using Pillow Python library.

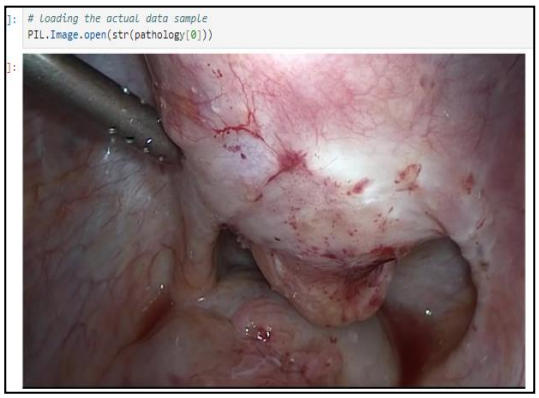

Fig. 2(a): Endometriosis (Non-Pathology)

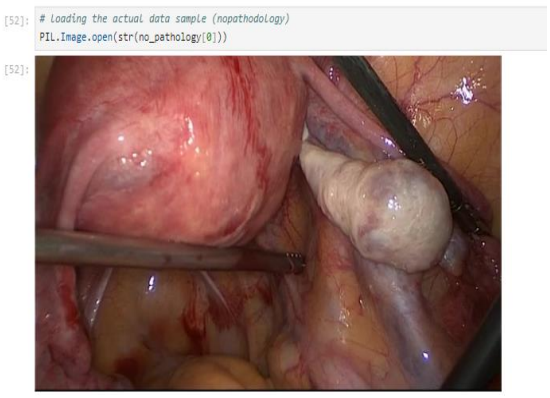

Fig. 2(b): Endometriosis (Pathology)

3.1.3 Preprocessing

The images used for training were resized to image input size of *224-by-224. The* pixel values was resized using rescale value of 1./255 to a common range between 0-1 to enhance the model training.To prevent over fitting as a result of our limited datasets, data augmentation was used to generate more training data from existing training samples, by augmenting the samples via a number of random transformations that produces images with similar properties to the existing images.This exposes the model to more aspects of the data and generalize better. A pre-trained convolutional neural network ResNet50v2 and it's origin (imageNet) was used for feature extraction. ResNet50V2(include_top=False) was used to exclude the final classification layers, focusing on extracting features from the intermediate layers. Because these layers capture valuable image representations learned from the large ImageNet dataset. The model was implemented using Keras in google colab pro environment. Model was trained in Google colab pro environment with high utilising GPU of 15 GB and a virtual RAM 13GB and 78GB of virtual disk space.

3.2 Endometriosis Models (CNN, VGG16, MobileNet, ResNet)

In this study, Endometriosis model was developed with one (1) DL based architecture CNN, and four (4) transfer learning CNN, VGG16, MobileNet, ResNet. CNN is a deep neural network to train the endometriosis classification model and, RestNet101V2, VGG16, and MobileNetV2 are the transfer learning architecture employed. This developed Endometriosis model was evaluated with accuracy, precision and recall performance metrics.Also, the model was bemchmarked with other existing models.comparative analysis. To get a good performance of the model Pelican Optimizer was used to extract the features with greatest importance. Table 1 presents the Optimized Endometriosis Classification model with Pelican Optimize.

Table 1: Optimized Endometriosis Classification model with Pelican Optimizer

INPUT: endometriosis_img
OUTPUT: Result ← ComparePerformance(Endometriosis_model, Accuracy, Precision, Recall).

START
INPUT: endometriosis_img ← Load from Kaggle().
Img_numpy_list = Load(endometriosis_img).
FOR each img in Img_numpy_list:
    resize_img = Img.resize(45, 80).
RETURN resize_img.
END FOR.
scaled_img = resize_img / 255.
train_img, test_img ← splitter_function(scaled_img, 80%, 20%).
Define models: {CNN, VGG16, MobileNet, ResNet}.
Initialize Pelican Optimization Algorithm:
Define hyperparameters search space:
Learning rate: [10−5,10−210^{-5}, 10^{-2}10−5,10−2]
Batch size: [16, 128]
Filters: [32, 256]
Dense units: [32, 256]
Initialize pelican population and objective function:
Objective function = Accuracy (to maximize accuracy).
FOR each model in models:
    Optimize model hyperparameters using POA:
    optimized_params = POA.run().
    Configure model with optimized_params.
    Endometriosis_model = Train(model, train_img, optimized_params).
    Accuracy, Precision, Recall ← Evaluate(Endometriosis_model, test_img).
    RETURN Endometriosis_model, Accuracy, Precision, Recall.
END FOR.
Result ← ComparePerformance(Endometriosis_model, Accuracy, Precision, Recall).
PRINT Result.
STOP

3.3 Pelican Optimization Algorithm (POA)

Firstly, it's essential to clone the Pelican Optimization Algorithm from the online Git repository. Then with the help of the PIP command, the Optimization Algorithm will be preinstalled within the Python Module. The Objective function for training the optimized deep learning model, and the Pelican Optimizer passing the objective function and search space configuration as parameter is defined. The search space denotes possible parameter combination set for the Optimizer selected for enhancing the performance of the endometriosis model classification. The parameter includes filters, dense unites, learning rates, and batch size.

3.4 Data Distribution

The exploration data analysis was conducted to observe the key features such as sample size of the data, the shape of the images, and visualizing images from each class, among other tasks. Furthermore, to graphically visualize the sample sizes for further exploration a bar chat is utilized for this exploration as shown in Fig 3. It shows the actual data sample of non-pathology samples of the endometriosis dataset.

`

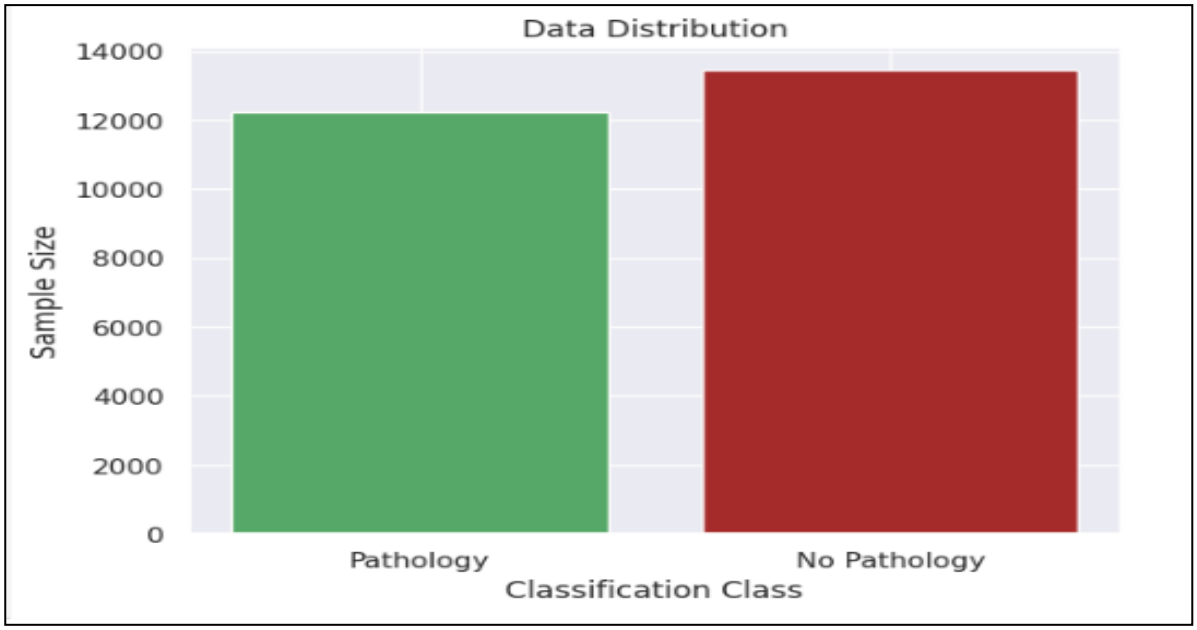

Fig. 3: Image Data Sample size Distribution

Fig.4 and Fig. 5 shows that the image samples of Pathology and No--pathplogy which depicts that Non-pathology sample is more compared to the Pathology image sample size, this minority difference will result into a model with minor or no biased prediction. A detailed basic image view in photo format will be used to explore the images from the different (pathology and non-pathology) class of the endometriosis dataset.

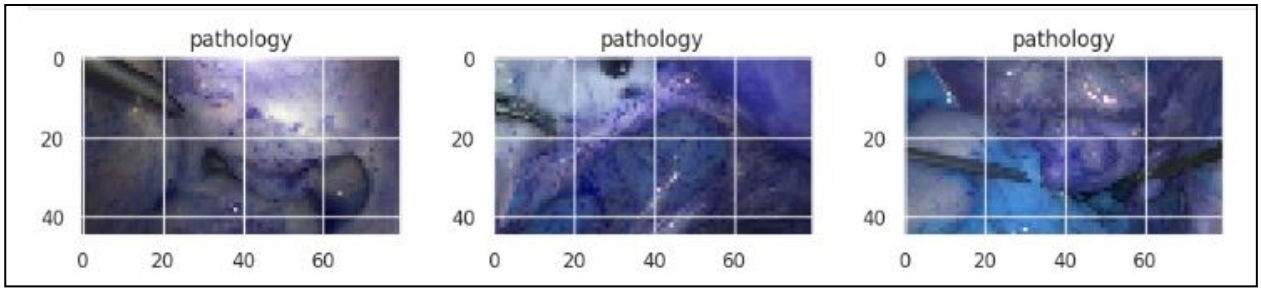

Fig. 4: Endometriosis (Pathology Sample Data)

Three image samples from Pathology classes are visualize in Fig.4. A similar pattern is visually observed by the naked eyes. Also, Fig.5 shows the three sample images from the No-pathology class.

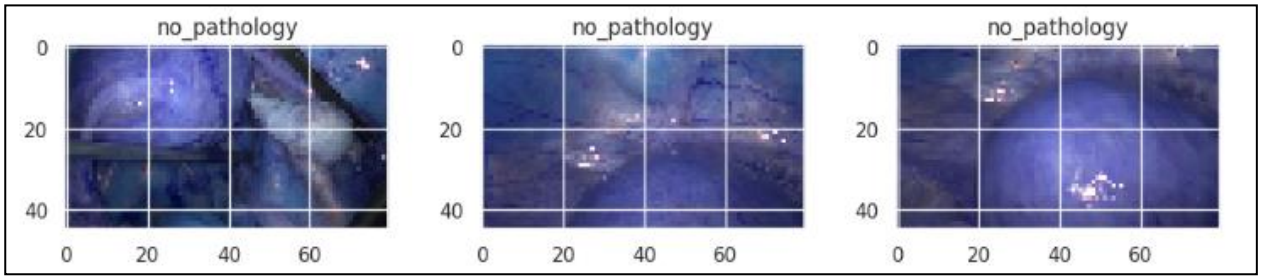

Fig. 5: Endometriosis (No-Pathology Sample Data)

Based on the Fig.5 the Non-Pathology samples are also similar in patterns that are visible to the human eyes. However, this pattern is automatically extracted by the deep learning model considered for training

4. RESULT/DISCUSSION

4.1. Endometriosis CNN Training

CNN Architecture is Sequential, with various keras layer such as the Input layer, Convolution 2-dimensional layer, a max-pooling layer, flatten layer and dense layer. The input layer accepts image shape of (45, 80, 3), which is specified using the *shape= (45,80,3)* parameter within the input layer of the sequential model. Next is the CNN layer consisting of two layers of convolution layer and max-pooling layer, the convolution layer helps in feature extraction using series of filter specified as *filters=32* parameter within the Conv2D layers. The max-pooling layers are included for dimensionality reductions immediately after the convolution operation on the inputted images.

Finally, the flatten layer and the Dense layer. Flatten layer is included in other to have a lower dimensional representation of the image extracted feature before passing them to the fully connected dense layer of 128 neurons and *relu* as the activation function. The last Dense layer denotes the output layer with a single neuron and sigmoid as the activation function. The last layer outputs a probability score of the image sample been *pathology* or *non-pathology*. The compilation parameter such as the loss metric set to binary_cross-entropy due to the binary classification problem, optimization parameter set to parameter, and lastly the accuracy evaluation metric is also specified. Table 2 shows the proposed CNN architecture summary.

Table 2: CNN Architecture Summary

Model: "sequential_4"

Layer (type)	Output Shape	Param #
conv2d_8 (Conv2D)	(None, 43, 78, 32)	896
max_pooling2d_8 (MaxPooling2D)	(None, 21, 39, 32)	0
conv2d_9 (Conv2D)	(None, 19, 37, 64)	18,496
max_pooling2d_9 (MaxPooling2D)	(None, 9, 18, 64)	0
flatten_4 (Flatten)	(None, 10368)	0
dense_8 (Dense)	(None, 128)	1,327,232
dense_9 (Dense)	(None, 1)	129

Total params: 1,346,753 (5.14 MB)
Trainable params: 1,346,753 (5.14 MB)
Non-trainable params: 0 (0.00 B)

4.2 Endometriosis Resnet101v2 Training

Resnet101v2 is a transfer learning-based architecture with very deep layers in its architectural definition. With the weight parameter, the pre-trained weight of ImageNet can be downloaded from their online repository, and the classification head can be removed by setting the RestNet include top parameter to False. Part of the Layer summary is shown in Table 3.

Table 3 shows the ResNet101V2 Architecture layout configuration without the classification head specified using *include_top=False* in the *ResNet101V2* parameter. The ImageNet pre-trained weight is considered and loaded into the architecture using the *weight* parameter been set to *imageNet.* This pre-trained ResNet weight is stored in a single variable called *resnet_weight* which will serve as a functional layer in the Endometriosis Transfer Learning Architecture. The input layer of the ResNet101V2 architecture is define using keras module, then the output of the input layer is passed as functional parameter t “o the *resnet* layer.

However, the ResNet layers are freezed (the weights are not updated during training), and the output are forwarded to the Dense layer. The First layer is a gl obal max pooling layer to convert the 3 dimensional data into a 2 dimensional output for the fully connected Dense layer. However, two dense layer are considered with 1,024 and 256 neurons and *relu* activation function. The last Dense layer denote the output layer with single neuron and sigmoid as the activation function. The last layer output a probability score of the image sample been *pathology*
or *non-pathology*. The compilation parameter such as the loss metric set to binary_crossentropy due to the binary classification problem, optimization parameter set to parameter, and lastly the accuracy evaluation metric is also specified. Table 4 shows the summary of the proposed Endometriosis RestNet101V2 based architecture.

Table 3: ResNet101V2 Pre-Trained Architecture Model

ResNet Model

```
# loading the resnet pre-trained model
resenet_weight = ResNet101V2(weights = 'imagenet', include_top = False)
resenet_weight.summary()
```

Model: "resnet101v2"

Layer (type)	Output Shape	Param #	Connected to
input_layer_7 (InputLayer)	(None, None, None, 3)	0	-
conv1_pad (ZeroPadding2D)	(None, None, None, 3)	0	input_layer_7[0]…
conv1_conv (Conv2D)	(None, None, None, 64)	9,472	conv1_pad[0][0]
pool1_pad (ZeroPadding2D)	(None, None, None, 64)	0	conv1_conv[0][0]
pool1_pool (MaxPooling2D)	(None, None, None, 64)	0	pool1_pad[0][0]
conv2_block1_preac… (BatchNormalizatio…	(None, None, None, 64)	256	pool1_pool[0][0]
conv2_block1_preac… (Activation)	(None, None, None, 64)	0	conv2_block1_pre…
conv2_block1_1_conv (Conv2D)	(None, None, None, 64)	4,096	conv2_block1_pre…
conv2_block1_1_bn (BatchNormalizatio…	(None, None, None, 64)	256	conv2_block1_1_c…
conv2_block1_1_relu (Activation)	(None, None, None, 64)	0	conv2_block1_1_b…
conv2_block1_2_pad (ZeroPadding2D)	(None, None, None, 64)	0	conv2_block1_1_r…
conv2_block1_2_conv (Conv2D)	(None, None, None, 64)	36,864	conv2_block1_2_p…
conv2_block1_2_bn (BatchNormalizatio…	(None, None, None, 64)	256	conv2_block1_2_c…
conv2_block1_2_relu (Activation)	(None, None, None, 64)	0	conv2_block1_2_b…

Table 4: Endometriosis ResNet101V2 Pre-Trained Architecture Summary

Model: "functional_6"

Layer (type)	Output Shape	Param #
input_layer_8 (InputLayer)	(None, 45, 80, 3)	0
resnet101v2 (Functional)	(None, 2, 3, 2048)	42,626,560
global_max_pooling2d_1 (GlobalMaxPooling2D)	(None, 2048)	0
dense_13 (Dense)	(None, 1024)	2,098,176
dense_14 (Dense)	(None, 256)	262,400
dense_15 (Dense)	(None, 1)	257

Total params: 44,987,393 (171.61 MB)

Trainable params: 44,889,729 (171.24 MB)

Non-trainable params: 97,664 (381.50 KB)

4.3 Endometriosis Mobilenet training

MobileNet is a transfer learning based architecture with very deep layers in is architectural definition. With the weight parameter, the pre-trained weight of Imagenet can be downloaded from their online repository and the

classification head can be removed by setting the MobileNet *include_top* parameter to False. Part of the Layer summary is shown in Table 5.

Table 5. MobileNet Pre-Trained Architecture

MOBILE Net Model

```
[21]: mobilenet_weight = MobileNet(weights = 'imagenet', include_top = False)
      mobilenet_weight.summary()
```

```
Downloading data from https://storage.googleapis.com/tensorflow/keras-applications/mobilenet/mobilenet_1_0_224_t
17225924/17225924 ━━━━━━━━━━━━━━━━━━━━ 1s 0us/step
Model: "mobilenet_1.00_224"
```

Layer (type)	Output Shape	Param #
input_layer_9 (InputLayer)	(None, None, None, 3)	0
conv1 (Conv2D)	(None, None, None, 32)	864
conv1_bn (BatchNormalization)	(None, None, None, 32)	128
conv1_relu (ReLU)	(None, None, None, 32)	0
conv_dw_1 (DepthwiseConv2D)	(None, None, None, 32)	288
conv_dw_1_bn (BatchNormalization)	(None, None, None, 32)	128
conv_dw_1_relu (ReLU)	(None, None, None, 32)	0
conv_pw_1 (Conv2D)	(None, None, None, 64)	2,048
conv_pw_1_bn (BatchNormalization)	(None, None, None, 64)	256
conv_pw_1_relu (ReLU)	(None, None, None, 64)	0
conv_pad_2 (ZeroPadding2D)	(None, None, None, 64)	0

Table 5. shows the MobileNet Architecture layout configuration without the classification head specified using *include_top=False* in the MobileNet parameter. The ImageNet pre-trained weight is considered and loaded into the architecture using the *weight* parameter been set to *imagenet.* This pre-trained MobileNet weight is stored in a single variable called *mobilenet_weight* which will serve as a functional layer in the proposed Endometriosis Transfer Learning Architecture. The input layer is defined using Keras module, then the output of the input layer is passed as functional parameter to the *mobilenet* layer. However, the MobileNet layers are freeze (the weights are not updated during training), and the output are forwarded to the Dense layer.

The First layer is a global max pooling layer utilize for converting the 3 dimensional data into a 2 dimensional output for the fully connected Dense layer. However, two dense layer are considered with 1,024 and 256 neurons and *relu* activation function. The last Dense layer denote the output layer with single neuron, and sigmoid as the activation function. The last layer output a probability score of the image sample being *pathology* or *non-pathology*. The compilation parameter such as the loss metric is set to binary_crossentropy due to the binary classification problem, optimization parameter, and lastly the accuracy evaluation metric is also specified. Table 6 shows the summary of the proposed Endometriosis MobileNet based architecture summary.

Table 6: MobileNet Endometriosis Pre-Trained Architecture Summary

Model: "functional_9"

Layer (type)	Output Shape	Param #
input_layer_12 (InputLayer)	(None, 45, 80, 3)	0
mobilenet_1.00_224 (Functional)	(None, 1, 2, 1024)	3,228,864
global_max_pooling2d_4 (GlobalMaxPooling2D)	(None, 1024)	0
dense_22 (Dense)	(None, 1024)	1,049,600
dense_23 (Dense)	(None, 256)	262,400
dense_24 (Dense)	(None, 1)	257

Total params: 4,541,121 (17.32 MB)

Trainable params: 4,519,233 (17.24 MB)

Non-trainable params: 21,888 (85.50 KB)

4.4 Endometriosis VGG16 training

VGG16 is a transfer learning-based architecture with very deep layers in is architectural definition. With the weight parameter the pre-trained weight of *Imagenet* can be downloaded from their online repository and the classification head can be removed by setting the VGG16 include_top parameter to False. Part of the Layer summary is shown in Table 7

Table 7 shows the VGG16 Architecture layout configuration without the classification head as specify using include_top=False in the VGG16 parameter. The ImageNet pre-trained weight is considered and loaded into the architecture using the weight parameter been set to imagenet. This pre-trained VGG16 weight is stored in a single variable called vgg16_weight which will serve as a functional layer in the proposed VGG16 Endometriosis Transfer Learning Architecture. The input layer is defined using Keras module, and the output of the input layer is passed as functional parameter to the *vgg16* layer. However, the VGG16 layers are freeze (the weights are not updated during training), and the output are forwarded to the Dense layer.

The First layer is a global max pooling layer utilize for converting the 3 dimensional data into a 2 dimensional output for the fully connected Dense layer. However, two dense layer are considered with 1,024 and 256 neurons and *relu* activation function. Lastly, the last Dense layer denote the output layer with single neuron, and sigmoid as the activation function. The last layer output a probability score of the image sample been pathology or non-pathology.

Table 7: VGG16 Pre-Trained Architecture

```
vgg_weight = vgg16.VGG16(weights = 'imagenet', include_top = False)
vgg_weight.summary()
```

Model: "vgg16"

Layer (type)	Output Shape	Param #
input_layer_27 (InputLayer)	(None, None, None, 3)	0
block1_conv1 (Conv2D)	(None, None, None, 64)	1,792
block1_conv2 (Conv2D)	(None, None, None, 64)	36,928
block1_pool (MaxPooling2D)	(None, None, None, 64)	0
block2_conv1 (Conv2D)	(None, None, None, 128)	73,856
block2_conv2 (Conv2D)	(None, None, None, 128)	147,584
block2_pool (MaxPooling2D)	(None, None, None, 128)	0
block3_conv1 (Conv2D)	(None, None, None, 256)	295,168
block3_conv2 (Conv2D)	(None, None, None, 256)	590,080
block3_conv3 (Conv2D)	(None, None, None, 256)	590,080
block3_pool (MaxPooling2D)	(None, None, None, 256)	0
block4_conv1 (Conv2D)	(None, None, None, 512)	1,180,160
block4_conv2 (Conv2D)	(None, None, None,	2,359,808

Table 8: further revealed the compilation parameters such as the loss metric set to binary_crossentropy due to the binary classification problem, optimization parameter set to parameter, and lastly the accuracy evaluation metric is also specified. Table 8 shows the summary of the proposed Endometriosis VGG16-based architecture summary.

Table 8: Endometriosis VGG16 Pre-Trained Architecture Summary

Model: "functional_18"

Layer (type)	Output Shape	Param #
input_layer_28 (InputLayer)	(None, 45, 80, 3)	0
vgg16 (Functional)	(None, 1, 2, 512)	14,714,688
global_max_pooling2d_13 (GlobalMaxPooling2D)	(None, 512)	0
dense_49 (Dense)	(None, 1024)	525,312
dense_50 (Dense)	(None, 256)	262,400
dense_51 (Dense)	(None, 1)	257

Total params: 15,502,657 (59.14 MB)

Trainable params: 787,969 (3.01 MB)

Non-trainable params: 14,714,688 (56.13 MB)

4.5 Findings of Research

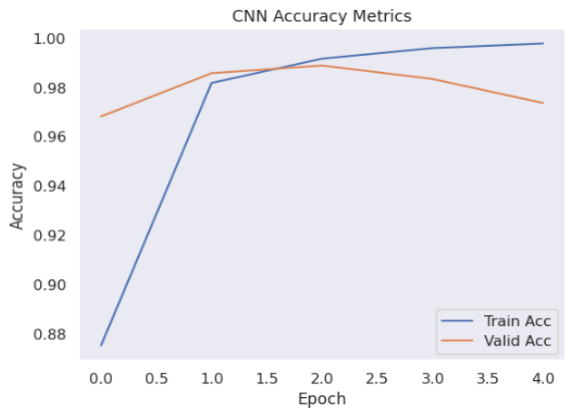

Fig. 6(a): CNN Training & Validation Accuracy

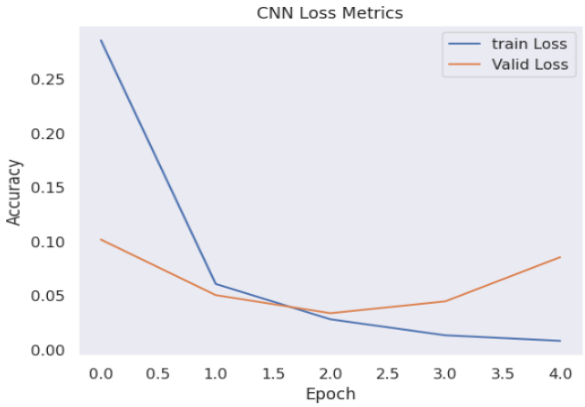

Fig. 6(b): CNN Training & Validation Loss

Fig.6(a) and (b) shows the training and validation curve of the CNN model Accuracy and loss performance during training and validation. Based on the curve the training progressively improved across the epochs, while validation diminished right from the 2nd iteration. The pattern is also observed from the loss metric. Furthermore, to collectively visualize the CNN performance the Classification report and confusion Matrix is visualize in Fig.7.

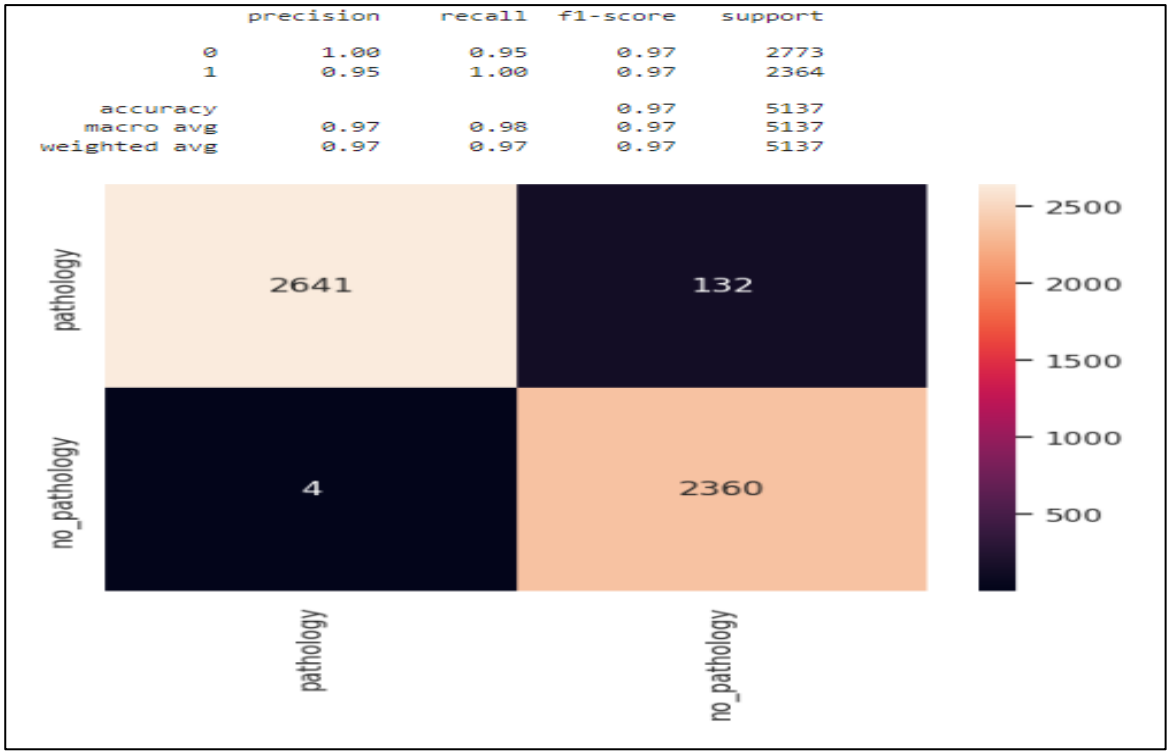

Fig. 7: CNN Classification Report and Confusion Matrix

CNN achieved a general accuracy of 97% for the detection of endometriosis as shown Fig.7:, thus the classification of pathology and non-pathology image sample. However, the precision score of 97.5%, Recall score of 97.5%, and F1-score of 97% is achieved using CNN architecture. The confusion matrix is also displayed in Fig.7: in other to achieve correct prediction and false prediction rate. Based on the confusion matrix, the model correctly classifies the *pathology* class 2,641 times and 132 time it miss-classifies, while 2,360 times, the model correctly classifies the *no_pathology* class, and miss-classified it 4 times.

4.6 ResNet101V2 performance evaluation

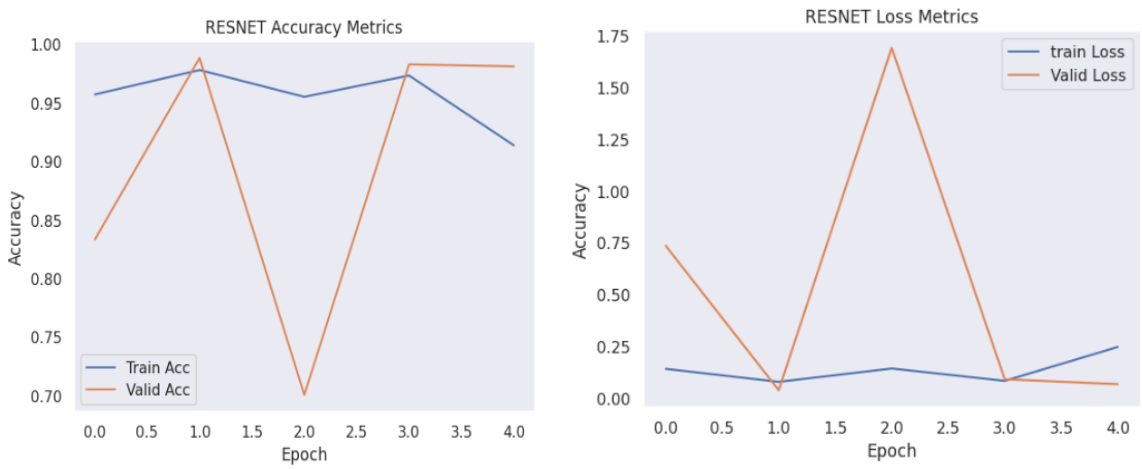

Fig. 8(a): ResNet101V2 Training & Validation Accuracy **Fig. 8(b):** ResNet101V2 Training & Validation Loss

Fig.8(a) and Fig.8(b) shows the training and validation curve of the ResNet101V2 model accuracy and loss performance during training and validation. Based on the curve there is high level of irregularity (zigzag pattern) observed on the validation data but very minimal in training data, and a little diminish in accuracy and loss. This same pattern is also observed from the loss metric. Furthermore, to collectively visualize the ResNet101V2 performance the Classification report and confusion Matrix is visualized in Fig. 9.

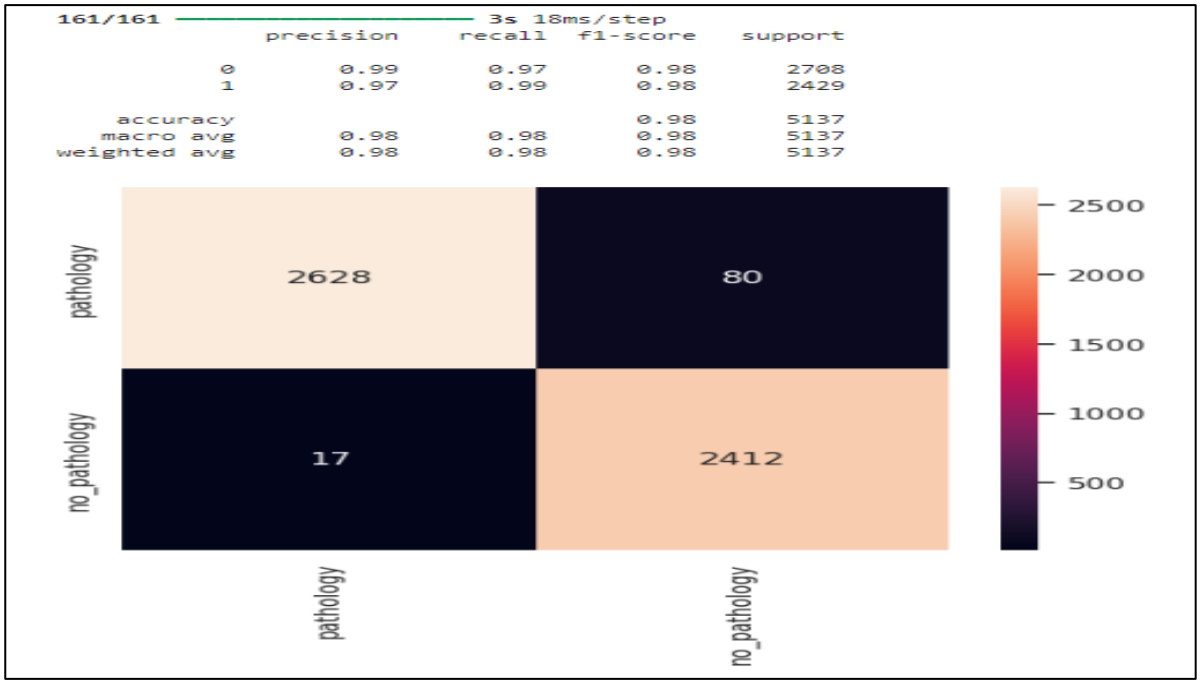

Fig. 9: ResNet101V2 Classification Report and Confusion Matrix

4.7 MobileNet performance evaluation

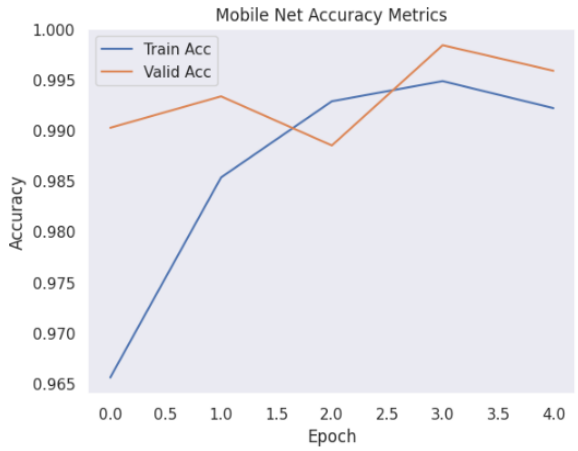

Fig. 10(a): MobileNet Training & Validation Accuracy

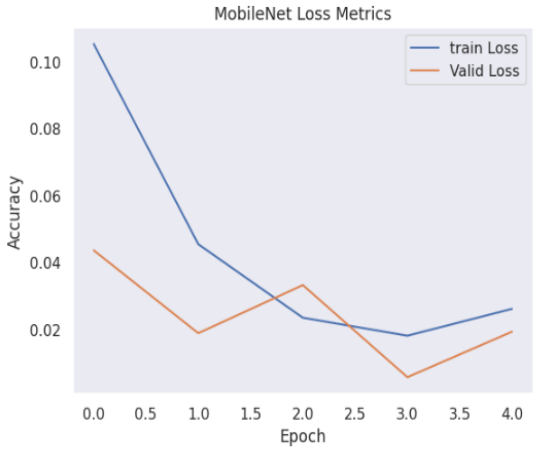

Fig.10 (b): MobileNet Training & Validation Loss

Fig.10(a) and Fig.10(b): shows the training and validation curve of the MobileNet model Accuracy and loss performance during training and validation. Based on the curve the training progressively improved across the epochs, while validation diminished has rough training pattern across each epoch. The pattern is also observed from the loss metric. Furthermore, to collectively visualize the MobileNet performance the Classification report and confusion Matrix is shown in Fig.11.

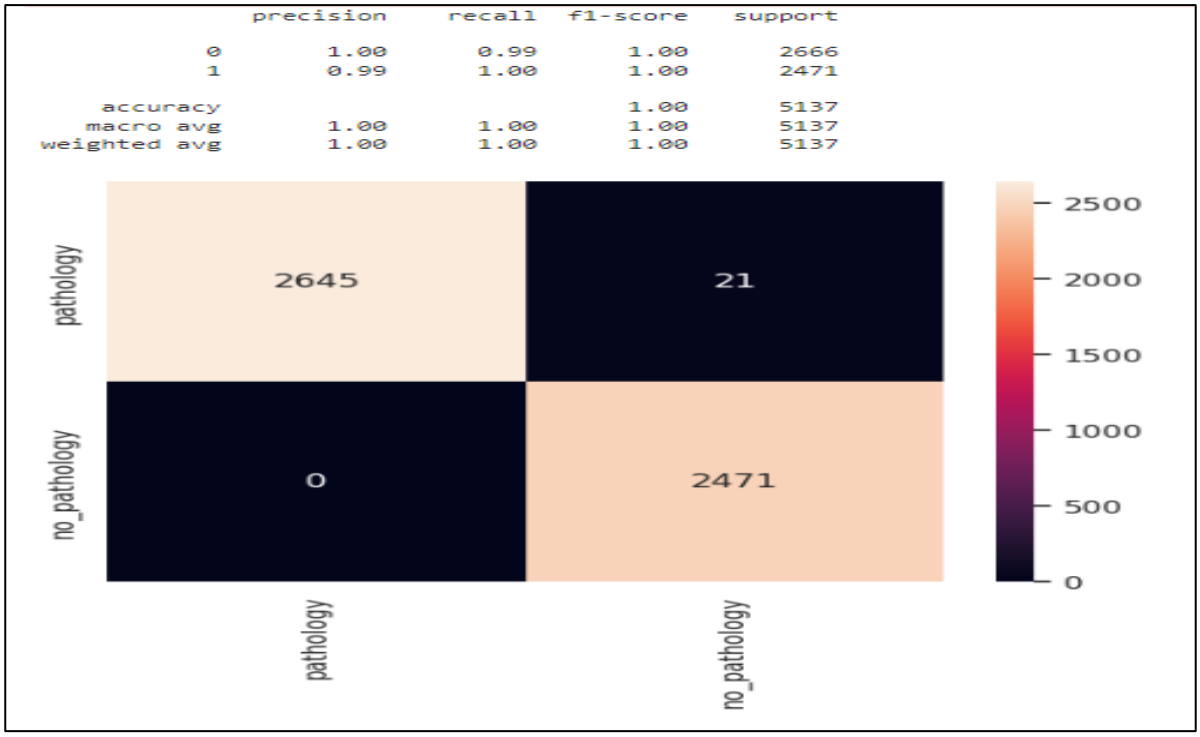

Fig. 11: MobileNet Classification Report Confusion Matrix

MobileNet achieved a general accuracy of 100% for the detection of endometriosis, as shown in Fig.11, thus the classification of pathology and non-pathology image sample. However, the precision score of 99.0%, the recall score of 99.0%, and F1-score of 100% is achieved using MobileNet architecture. Lastly, the confusion matrix for MobileNet obtain correct prediction and false prediction rate. Based on the confusion matrix, 2,645 are classified correctly as *pathology* case and 21 is miss-classified, while 2,471 are correctly classified as no pathology cases, and 0 are miss-classified. The VGG16 Classification Report & Confusion Matrix is shown in Fig. 12.

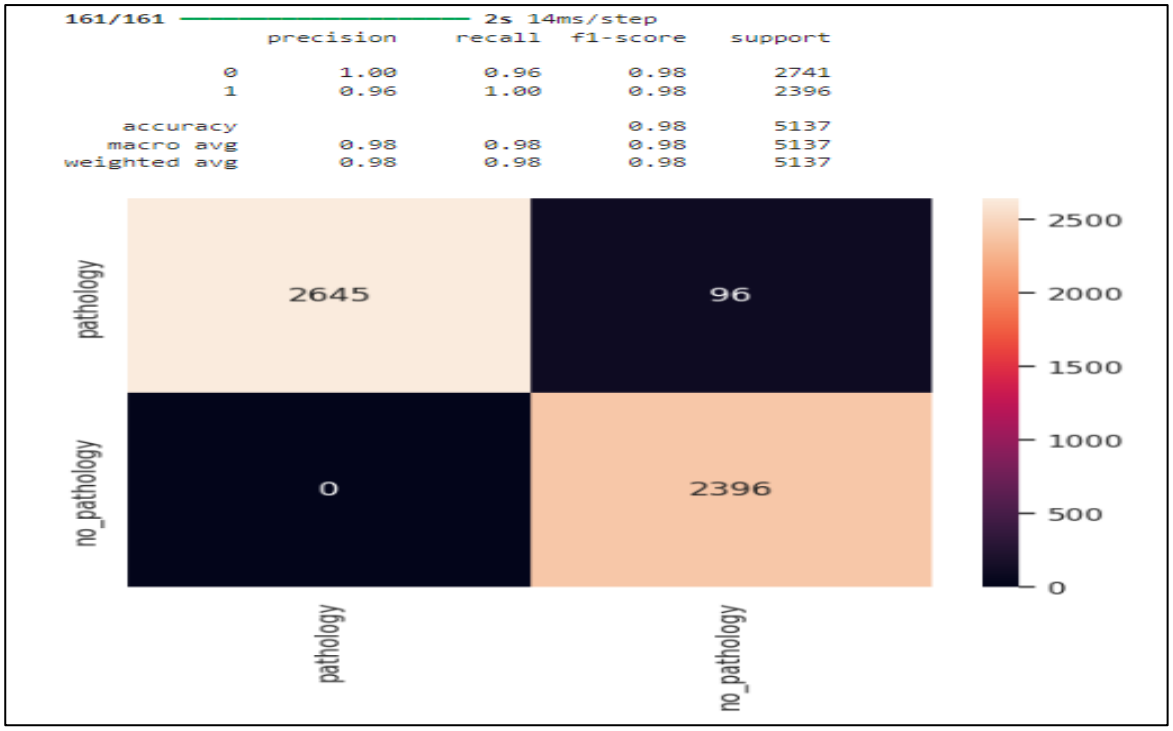

Fig. 12: VGG16 Classification Report & Confusion Matrix

To collectively visualize the VGG16 performance the Classification report and confusion Matrix is shown in Fig.12. VGG16 achieved a general accuracy of 100% for the detection of endometriosis as shown in Fig.12, thus the classification of pathology and non-pathology image sample. However, the precision score of 96.0%, Recall score of 96.0%, and F1-score of 98% is achieved using VGG16 architecture. Lastly, the confusion matrix for VGG16 obtain correct prediction and false prediction rate. Based on the confusion matrix, 2,645 are correctly classified as *pathology* cases and ninety six (96) are miss-classified, while 2,396 are correctly classified as*no_pathology* class, and miss-classified is zero (0). The training and validation curve of the VGG16 model is shown in Fig. 13(a) anf Fig. 13(b).

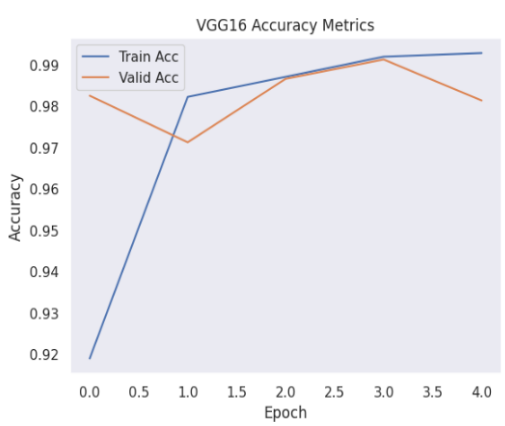

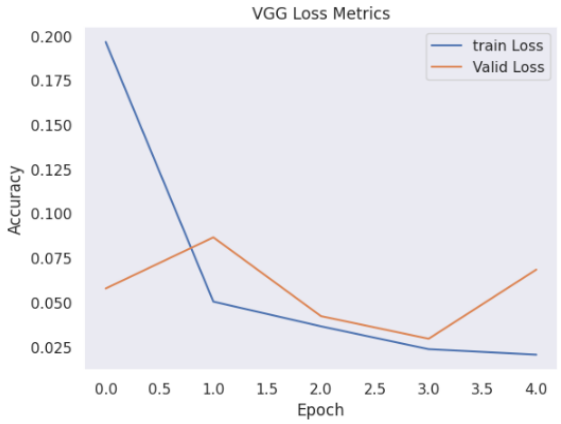

Fig. 13(a): VGG16 Training & Validation Accuracy

Fig.13 (b): VGG16 Training & Validation Loss

Fig.13(a) and Fig 13(b): show the training and validation curve of the VGG16 model accuracy and loss performance during training and validation. Based on the curve shown, the training progressively improved across the epochs, while validation diminished as rough training pattern across each epoch. The pattern is also observed from the loss metric.

4.7 Endometriosis & POA Classification Report

The CNN & POA confusion matrix is shown in Fig. 14, while ResNet101V2 & POA is shown in Fig. 15 as VGG16 & POA is shown Fig.16, and MobileNet & POA is also shown in Fig. 17.

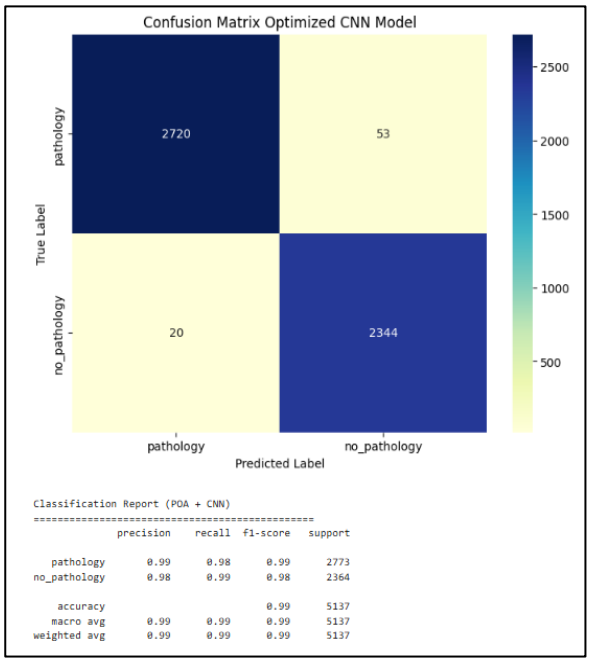

Fig. 14: CNN & POA

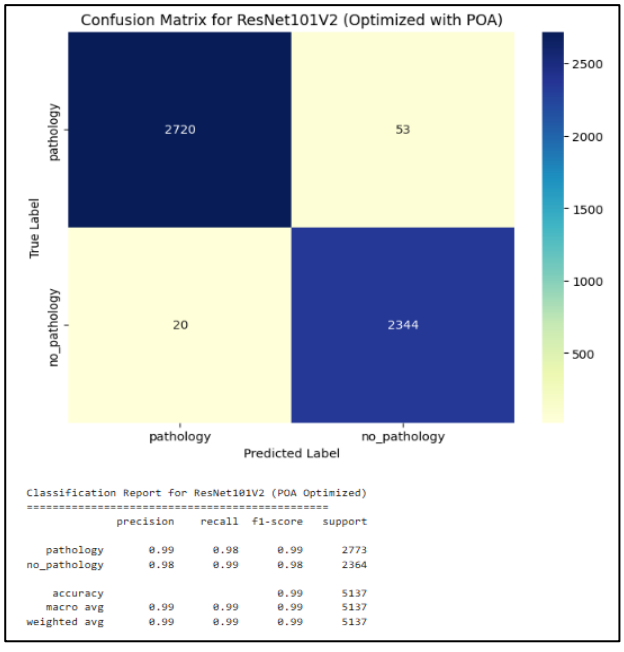

Fig. 15: ResNet101V2 & POA

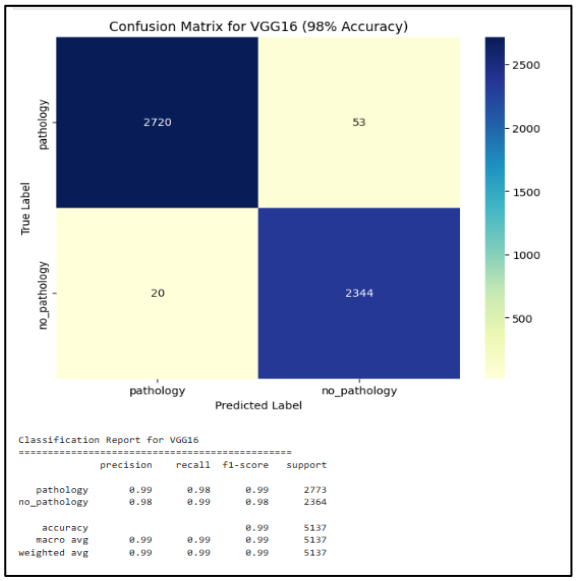

Fig. 16: VGG16 & POA

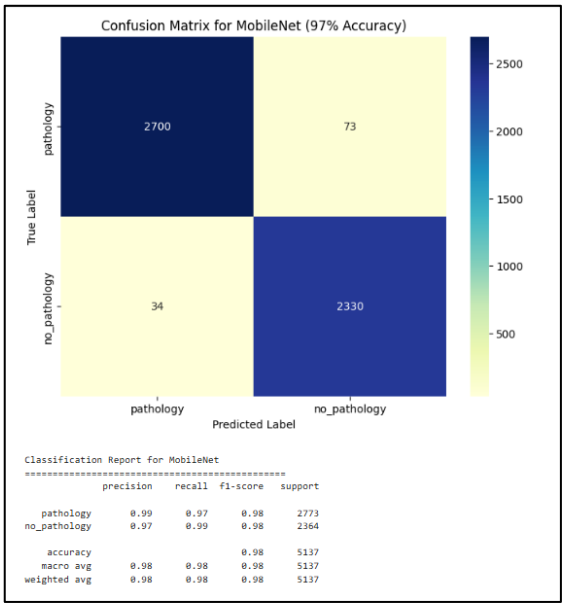

Fig. 17: MobileNet & POA

Fig.14, Fig.15, Fig.16 and Fig.17 show the confusion matrix and classification report of the Optimized CNN, VGG16, ResNet101V2 and MobileNet. The results shows that the model obtains an accuracy of 98%, 98%, 99%, and 97% respectively.

4.9 Comparative Analysis

This section introduces the comparative analysis between the proposed CNN, RestNet101V2, MobileNet, and VGG16 and the Pelican based Optimized version of the classification model. Finally, the proposed models will be compared with existing work on the same endometriosis classification.

Table 9: Model Performance Comparison

S/N	Model	Accuracy	Precision	Recall	F1-Score
1	CNN	97%	100%	95%	97%
			95%	100%	97%
2	ResNet101V2	98%	99%	97%	98%
			97%	99%	98%
3	MobileNet	100%	100%	99%	100%
			99%	100%	100%
4	VGG16	98%	100%	96%	98%
			96%	100%	98%
5	CNN + POA	98%	99%	98%	98%
			98%	99%	98%
6	ResNet101V2 + POA	99%	99%	98%	98%
			98%	99%	98%
7	MobileNet + POA	97%	100%	97%	98%
			97%	100%	98%
8	VGG16 + POA	98%	100%	97%	98%
			97%	100%	98%

Table 9 shows the comparative results between the proposed model, including the CNN, ResNet, MobileNet, and VGG16. Based on the Table 9 MobileNet attained the highest accuracy of 100% without the integration of POA, thus an overfitted model, while the Convolutional Neural Network with MobilNet+POA attained the lowest accuracy of 97%. Each performance for individual models and classes based on Precision, Recall, and F1-score is also summarized in the table. The Table 9 result is shown in Fig.18, Fig.19 and Fig. 20.

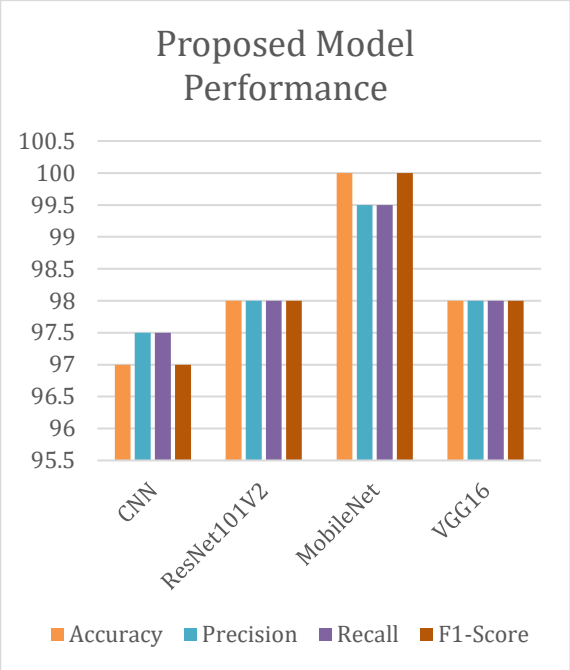

Fig. 18: Model Performance Results

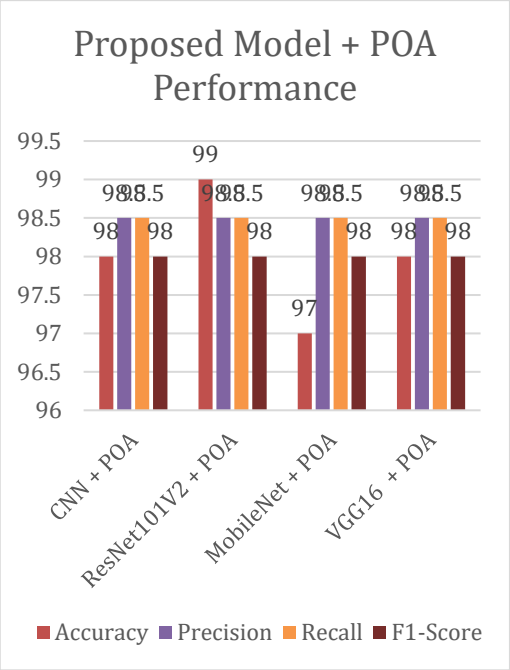

Fig. 19: Model Performance with Pelican Optimizer

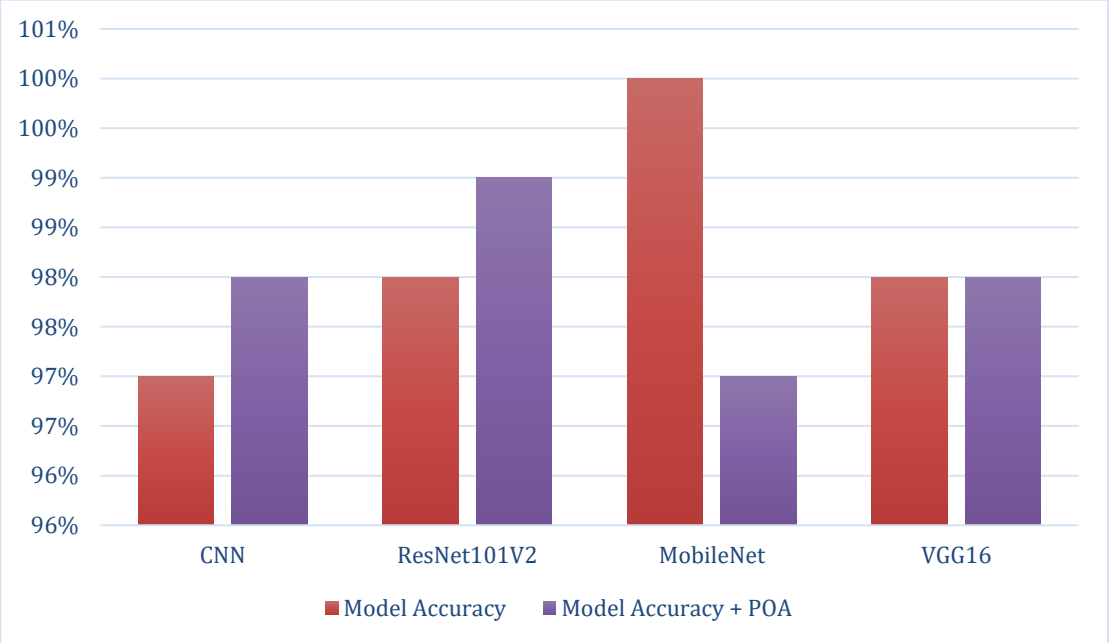

Fig. 20: Model Accuracy (Benchmark Model & Optimized Model)

Fig. 20: show the Optimizer address overfitting issue identified in the existing benchmark model. however, on an average threshold the Pelican Optimized Model performance efficiently that the benchmarked model (model with no optimized parameter tuning). The Optimized Model & Existing Model Comparison is presented in Table 10.

Table 10: Optimized Model & Existing Model Comparison

S/N	Author	Dataset	Data Sample Size	Model	Accuracy
1	Proposed, 2024	GLENDA_V1.0 (80%, 20%)	25,682	CNN	98%
2	Proposed, 2024	GLENDA_V1.0 (80%, 20%)	25,682	ResNet101V2	99%
3	Proposed, 2024	GLENDA_V1.0 (80%, 20%)	25,682	MobileNet	97%
4	Proposed, 2024	GLENDA_V1.0 (80%, 20%)	25,682	VGG16	98%
5	(Visalaxi & Muthu, 2021b)	GLENDA (60%, 40%)	6,000	VGG16	80%
6	(Visalaxi & Muthu, 2021b)	GLENDA (60%, 40%)	6,000	ResNet50	91%
7	(Visalaxi & Muthu, 2021b)	GLENDA (60%, 40%)	6,000	Inception ResNetV2	88%

Table 10 shows a result comparison between the proposed optimized POA model and the work of Visalaxi & Muthu, (2021). The accuracy performance, the different dataset utilizes, and the training/testing size are all summarize in table 4.2. This study utilizes 80% for training and 20% for validation, while the existing study considered 60% for training and 40% endometriosis sample for testing. However, considering the data sample size utilized by the existing study (6,000), is smaller compared to that of the image sample size utilized in this study (25,682). This difference in sample size contributed to the performance increase in the proposed architectures. Fig.20 shows a graphical visual of Table 10.

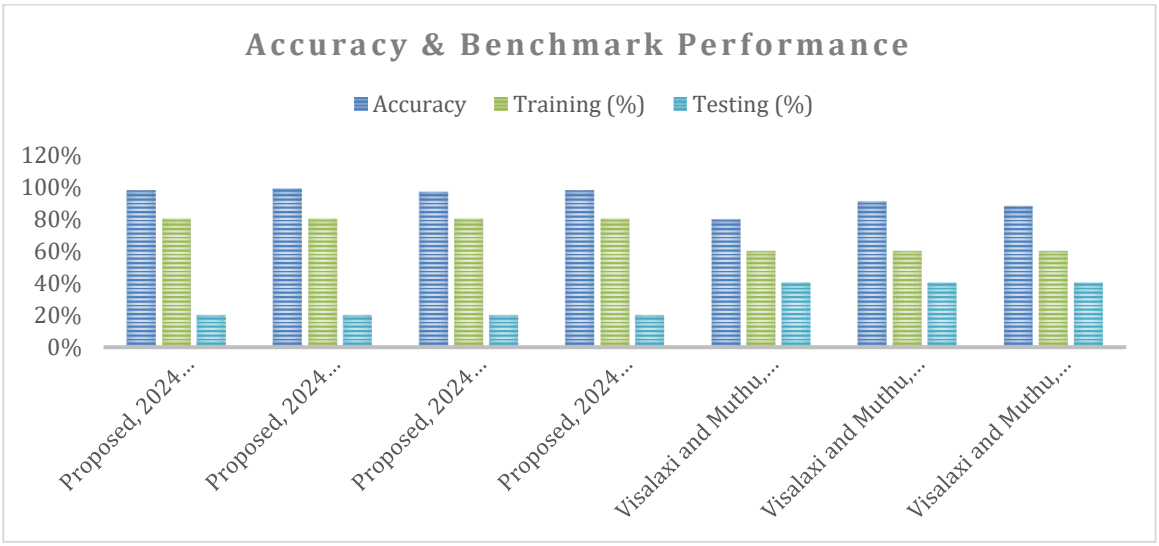

Fig. 20: Proposed Optimized Model & Existing Model Comparison

The accuracy difference, training size, and testing data size of the existing and proposed Optimized deep learning model are shown in Fig.20. Hence, the comparative study shows that the proposed POA model performs more efficiently than the existing study, taking advantage of larger dataset sample sizes.

4.10 Discussion

The research work primary focus on the development of endometriosis classification model using deep learning and transfer learning based techniques. Based on the extensive review conducted, limited attention has been to the enhancement and development of endometriosis classification models. However, other studies suffer from poor performance due to limited dataset samples for training. Hence, this study aims to develop an endometriosis prediction model for predicting if a patient is pathological or not pathological by utilizing four different deep/transfer learning architectures, including CNN, RestNet101V2, MobileNet, and VGG16. After development an extensive comparative analysis is conducted to properly evaluate the performance of the

developed prediction model. A comprehensive study is conducted to re-view similar work within the same research domain, in other to identify recent research gaps or novel techniques utilized and suggested by developer for enhancing model development. Furthermore, the research methodological approach is introduced after the comprehensive review, and various conceptual illustrations are designed using Microsoft Visio. The Conceptual design framework which reveals the entire idea about the system, flowchart diagram, and use case diagram for denoting the use case instance. The development take place within the Kaggle jupyter notebook environment for easy access to remote processing resources such as GPU and TPU. After development, a proper performance evaluation is performed using performance metrics such as accuracy, precision, f1-score and Recall. In conclusion the performance of the proposed system outperformed the existing work and benchmark CNN approach.

5. CONCLUSION

An extensive study was conducted on the utilization of deep learning/ transfer learning architectures for training endometriosis classification model. The experimental analysis conducted identified that transfer learning techniques (ResNet101V2, MobileNet, and VGG16) perform more efficiently better than deep learning (CNN) during the classification of endometriosis (pathology and non-pathology). However, comparative analysis with the existing study also revealed that more data samples improved the endometriosis detection and classification rate. Hence, the utilization of transfer learning approaches and the adoption of larger training samples can foster and enhance classification rate in the domain of endometriosis classification. In conclusion, the performance of the proposed system outperformed the existing work and the benchmark CNN approach. Further studies can be extended by considering more transfer learning architectures, and conduct a comparative analysis based on different parameter tuning, data sample size, and training epochs. For real time application or prediction of endometriosis classification, flask API can be utilized to create an application endpoint for professional and the general masses usage.

Declaration

Ethical Statement: The authors of this paper hereby give declaration of competing interest that this paper is our original work and has not been published in any media
Competing Interest: This article has no competing interests
Funding: There is no external funding received by the authors
Availability of data and material: http://ftp.itec.aau.at/datasets/GLENDA/v1_0/index.html
Consent to participate: Not Applicable

REFERENCES

1. Ghiasi, Marzieh, Madhavi Thombre Kulkarni, and Stacey A. Missmer. "Is endometriosis more common and more severe than it was 30 years ago?." *Journal of minimally invasive gynecology* 27, no. 2 (2020): 452-461.
2. K. Dagar and H. D. Ramteke, “Endometriosis: A systemic review,” Feb. 2023, doi: https://doi.org/10.13140/RG.2.2.27664.28164.
3. B. Smolarz, K. Szyłło, and H. Romanowicz, “Endometriosis: Epidemiology, Classification, Pathogenesis, Treatment and Genetics (Review of Literature),” *International Journal of Molecular Sciences*, vol. 22, no. 19, p. 10554, Sep. 2021, doi: https://doi.org/10.3390/ijms221910554.
4. J. Maddern, L. Grundy, J. Castro, and S. M. Brierley, “Pain in Endometriosis,” *Frontiers in Cellular Neuroscience*, vol. 14, no. 14, Oct. 2020, doi: https://doi.org/10.3389/fncel.2020.590823.
5. A. Goldstein and S. Cohen, “Self-report symptom-based endometriosis prediction using machine learning,” *Scientific Reports*, vol. 13, no. 1, Apr. 2023, doi: https://doi.org/10.1038/s41598-023-32761-8.
6. V. Kaul, S. Enslin, and S. A. Gross, “History of artificial intelligence in medicine,” *Gastrointestinal Endoscopy*, vol. 92, no. 4, pp. 807–812, Oct. 2020, doi: https://doi.org/10.1016/j.gie.2020.06.040.
7. D. Dahiwade, G. Patle, and E. Meshram, “Designing Disease Prediction Model Using Machine Learning Approach,” *IEEE Xplore*, Mar. 01, 2019. https://ieeexplore.ieee.org/document/8819782
8. K. Pingale, S. Surwase, V. Kulkarni, S. Sarage, and Prof. A. Prof. Abhijeet, “Disease Prediction Using Machine Learning,” *International Research Journal of Engineering and Technology (IRJET)*, vol. 06, no. 12, pp. 831–833, Dec. 2019.

`

9. M. El-flahgy, W. El-Bassioune, and W. Ayad, "Incidence of Endometriosis among Women Prepared for Laparoscopy in Unexplained Infertility and Chronic Pelvic Pain," *International Journal of Medical Arts*, vol. 0, no. 0, Jun. 2020, doi: https://doi.org/10.21608/ijma.2020.22163.1080.
10. S. A. Missmer *et al.*, "Impact of Endometriosis on Life-Course Potential: a Narrative Review," *International Journal of General Medicine*, vol. Volume 14, no. 14, pp. 9–25, Jan. 2021, doi: https://doi.org/10.2147/ijgm.s261139.
11. S. Simoens, L. Hummelshoj, and T. D'Hooghe, "Endometriosis: cost estimates and methodological perspective," *Human Reproduction Update*, vol. 13, no. 4, pp. 395–404, Jul. 2007, doi: https://doi.org/10.1093/humupd/dmm010.
12. J. V. Cardoso *et al.*, "Epidemiological profile of women with endometriosis: a retrospective descriptive study," *Revista Brasileira de Saúde Materno Infantil*, vol. 20, no. 4, pp. 1057–1067, Dec. 2020, doi: https://doi.org/10.1590/1806-93042020000400008.
13. S. Swain and P. K. Jena, "Diagnostic and Therapeutic Laparoscopy in the Management of Endometriosis," *International Journal of Reproduction, Contraception, Obstetrics and Gynecology*, vol. 7, no. 11, p. 4695, Oct. 2018, doi: https://doi.org/10.18203/2320-1770.ijrcog20184532.
14. C. Nezhat and Schipper, "Video-assisted Laparoscopy for the Detection and Diagnosis of endometriosis: safety, reliability, and Invasiveness," *International Journal of Women's Health*, p. 383, Jul. 2012, doi: https://doi.org/10.2147/ijwh.s24948.
15. G. Eleje, "Endometriosis Seen at Diagnostic Laparoscopy for Women with Infertility," *Journal of Gynecological Research and Obstetrics*, vol. 1, no. 1, pp. 006–009, Aug. 2015, doi: https://doi.org/10.17352/jgro.000002.
16. S Visalaxi and T Sudalai Muthu, "Automated prediction of endometriosis using deep learning," vol. 12, no. 2, pp. 2403–2416, Jul. 2021, doi: https://doi.org/10.22075/ijnaa.2021.5383.
17. X.-X. Yin, L. Sun, Y. Fu, R. Lu, and Y. Zhang, "U-Net-Based Medical Image Segmentation," *Journal of Healthcare Engineering*, vol. 2022, p. 4189781, Apr. 2022, doi: https://doi.org/10.1155/2022/4189781.
18. S. Dargan, M. Kumar, M. R. Ayyagari, and G. Kumar, "A Survey of Deep Learning and Its Applications: A New Paradigm to Machine Learning," *Archives of Computational Methods in Engineering*, Jun. 2019, doi: https://doi.org/10.1007/s11831-019-09344-w.
19. A. Sabat-Tomala, E. Raczko, and B. Zagajewski, "Comparison of Support Vector Machine and Random Forest Algorithms for Invasive and Expansive Species Classification Using Airborne Hyperspectral Data," *Remote Sensing*, vol. 12, no. 3, p. 516, Feb. 2020, doi: https://doi.org/10.3390/rs12030516.
20. V. Sankaravadivel and S. Thalavaipillai, "Symptoms based endometriosis prediction using machine learning," *Bulletin of Electrical Engineering and Informatics*, vol. 10, no. 6, pp. 3102–3109, Dec. 2021, doi: https://doi.org/10.11591/eei.v10i6.3254.
21. A. Goldstein and S. Cohen, "Self-report symptom-based endometriosis prediction using machine learning," *Scientific Reports*, vol. 13, no. 1, Apr. 2023, doi: https://doi.org/10.1038/s41598-023-32761-8.
22. A. Balica *et al.*, "Augmenting endometriosis analysis from ultrasound data using deep learning," Apr. 2023, doi: https://doi.org/10.1117/12.2653940.
23. S. Visalaxi and T. Sudalaimuthu, "Automated segmentation of endometriosis using transfer learning technique," *F1000Research*, vol. 11, p. 360, Mar. 2022, doi: https://doi.org/10.12688/f1000research.110283.1.
24. A. Leibetseder, K. Schoeffmann, J. Keckstein, and S. Keckstein, "Endometriosis detection and localization in laparoscopic gynecology," *Multimedia Tools and Applications*, vol. 81, no. 5, pp. 6191–6215, Jan. 2022, doi: https://doi.org/10.1007/s11042-021-11730-1.
25. P. Hu, Y. Gao, Y. Zhang, and K. Sun, "Ultrasound image-based deep learning to differentiate tubal-ovarian abscess from ovarian endometriosis cyst," *Frontiers in Physiology*, vol. 14, Feb. 2023, doi: https://doi.org/10.3389/fphys.2023.1101810.
26. F. S. Nahm, "Receiver Operating Characteristic curve: Overview and Practical Use for Clinicians," *Korean Journal of Anesthesiology*, vol. 75, no. 1, pp. 25–36, Feb. 2022, doi: https://doi.org/10.4097/kja.21209.
27. H. Zhang, "Machine Vision: A Comprehensive Analysis of Techniques, Applications, and Challenges," *Highlights in science, engineering and technology*, vol. 71, pp. 299–304, Nov. 2023, doi: https://doi.org/10.54097/hset.v71i.13050.
28. M. Rahimzadeh and A. Attar, "A modified deep convolutional neural network for detecting COVID-19 and pneumonia from chest X-ray images based on the concatenation of Xception and ResNet50V2," *Informatics in Medicine Unlocked*, vol. 19, p. 100360, 2020, doi: https://doi.org/10.1016/j.imu.2020.100360.

29. Djarot Hindarto, “Use ResNet50V2 Deep Learning Model to Classify Five Animal Species,” *Jurnal JTIK (Jurnal Teknologi Informasi dan Komunikasi)*, vol. 7, no. 4, pp. 758–768, Dec. 2023, doi: https://doi.org/10.35870/jtik.v7i4.1845.
30. Nisnab Udas, F. Beuth, and D. Kowerko, “Concept Detection in Medical Images using Xception Models - TUCMC at ImageCLEFmed 2020.,” *CLEF (Working Notes)*, Jan. 2020.
31. X. Yu, N. Zeng, S. Liu, and Y.-D. Zhang, “Utilization of DenseNet201 for diagnosis of breast abnormality,” *Machine Vision and Applications*, vol. 30, no. 7–8, pp. 1135–1144, Jul. 2019, doi: https://doi.org/10.1007/s00138-019-01042-8.
32. R. Anand, V. Sowmya, Vijaykrishnamenon, E. A. Gopalakrishnan, And K. P. Soman, “Modified Vgg Deep Learning Architecture For Covid-19 Classification Using Bio-Medical Images,” *IOP Conference Series: Materials Science and Engineering*, vol. 1084, no. 1, p. 012001, Mar. 2021, doi: https://doi.org/10.1088/1757-899x/1084/1/012001.
33. Ikegwu, A. C., Onyilo, J., & Nweke, H. F. (2025). Artificial intelligence-based clinical decision support systems: enhancing modern healthcare for smart diagnosis and prognosis. *Nat J Emerging Sci Technol Innovations*, *1*(1), 17-34.
34. Lee, S. Y., Koo, Y. J., & Lee, D. H. (2021). Classification of endometriosis. *Yeungnam University journal of medicine*, *38*(1), 10-18.
35. Pašalić, E., Tambuwala, M. M., & Hromić-Jahjefendić, A. (2023). Endometriosis: Classification, pathophysiology, and treatment options. *Pathology-Research and Practice*, *251*, 154847.
36. Condous, G., Gerges, B., Thomassin-Naggara, I., Becker, C. M., Tomassetti, C., Krentel, H., ... & Hudelist, G. (2024). Non-invasive imaging techniques for diagnosis of pelvic deep endometriosis and endometriosis classification systems: an International Consensus Statement. *Human Reproduction Open*, *2024*(3), hoae029.
37. Keckstein, J., & Hudelist, G. (2021). Classification of deep endometriosis (DE) including bowel endometriosis: From r-ASRM to# Enzian-classification. *Best practice & research Clinical obstetrics & gynaecology*, *71*, 27-37.
38. Missmer, S., Abrao, M. S., Einarsson, J. I., Horne, A. W., ... & De Wilde, R. L. (2022). International Working Group of AAGL, ESGE, ESHRE and WES, Zondervan, K. T., Endometriosis classification systems: an international survey to map current knowledge and uptake. *Human Reproduction Open*, *2022*(1), hoac002.
39. Bazot, Marc, Emile Daraï, Giuseppe P. Benagiano, Caroline Reinhold, Amelia Favier, Horace Roman, Jacques Donnez, and Sofiane Bendifallah. "ENDO_STAGE magnetic resonance imaging: classification to screen endometriosis." *Journal of clinical medicine* 11, no. 9 (2022): 2443.
40. Maciel, C., Ferreira, H., Djokovic, D., Kyaw Tun, J., Keckstein, J., Rizzo, S., & Manganaro, L. (2023). MRI of endometriosis in correlation with the# Enzian classification: applicability and structured report. *Insights into Imaging*, *14*(1), 120

`